Chest X-ray features facilitate screening for pulmonary hypertension caused by fibrosing mediastinitis

Mingfang Zhou*, Bo Li* (ID)**, Yaling Chen, Aqian Wang, Yining Zhu, Yu Li, Hongling Su, Jingchun Fan, Yan Zhang and Yunshan Cao** (ID)

Abstract

Background: Misdiagnosis and underdiagnosis of pulmonary hypertension caused by fibrosing mediastinitis (PH-FM) are considerably prevalent due to unspecific symptoms and as well as the lack of awareness of this fatal disease.

Objectives: The aim of this study was to evaluate the diagnostic accuracy of the chest X-ray (CXR) for screening the patients with PH-FM from those with pulmonary hypertension (PH).

Design: This was a retrospective observational cohort study.

Methods: The patients with suspected PH were recruited between October 2014 and October 2020. All the clinical data and CXR findings were collected. The sensitivity, specificity, and likelihood ratio of the CXR features were calculated. Logistic regression was used to identify the factors associated with the CXR characteristics and FM and to generate a prediction model. Finally, the diagnostic efficiency of the prediction model was evaluated using nomogram and internal validation.

Results: The patients with PH-FM ($n = 36$) and PH caused by the diseases other than FM (PH-non-FM, $n = 62$) were enrolled. The CXR features, including atelectasis, pleural effusion, consolidation, nodules, calcification, interlobular septal thickening, and interstitial reticulation, were more prevalent in patients with PH-FM than in those with PH-non-FM (all $p < 0.05$). Atelectasis had a specificity of 97%, a sensitivity of 50%, and a greater accuracy for diagnosing of PH-FM [area under the curve (AUC) = 0.720; 95% CI: 0.634–0.806] than the other factors did. The combination of tuberculosis, natural logarithmic NT-proBNP (lnBNP), atelectasis, pleural effusion, and prominent right heart border constituted a prediction model to distinguish the PH-FM from the PH-non-FM, with a sensitivity of 91.7% and a specificity of 83.9%. The model demonstrated good prediction performance by showing an AUC of 0.922 (95% CI: 0.861–0.983) in the internal validation.

Conclusion: In this study, atelectasis was the most specific and accurate CXR characteristic for identifying PH-FM in the PH patients. The combination of atelectasis, pleural effusion, prominent right heart border, tuberculosis, and lnBNP constituted a prediction model that distinguished the PH-FM patients from the PH-non-FM ones with good performance.

Keywords: atelectasis, chest X-ray, diagnosis, fibrosing mediastinitis, pulmonary hypertension, right heart failure

Correspondence to:
Yunshan Cao
Department of Cardiology, Pulmonary Vascular Disease Center (PVDC), Gansu Provincial Hospital, No. 204, Donggang West Road, Chengguan District, Lanzhou 730000, China.
yunshancao@126.com

Yan Zhang
Tianjin Key Laboratory of Retinal Functions and Diseases, Tianjin Branch of National Clinical Research Center for Ocular Disease, Eye Institute and School of Optometry, Tianjin Medical University Eye Hospital, 251, Fukang Road, Nankai District, Tianjin, China.
yanzhang04@tmu.edu.cn

Mingfang Zhou
Bo Li
Yaling Chen
The First Clinical Medical College of Gansu University of Chinese Medicine (Gansu Provincial Hospital), Lanzhou, China

Aqian Wang
Hongling Su
Department of Cardiology, Pulmonary Vascular Disease Center (PVDC), Gansu Provincial Hospital, Lanzhou, China

Yining Zhu
School of Mathematical Sciences, Fudan University, Shanghai, China

Yu Li
Department of Radiology, The Seventh Affiliated Hospital of Sun Yat-sen University, Shenzhen, China

Jingchun Fan
Gansu University of Chinese Medicine, Lanzhou, China

*Mingfang Zhou and Bo Li contributed equally.

Introduction

Pulmonary hypertension caused by fibrosing mediastinitis (PH-FM), belonging to group 5 of the World Health Organization PH classification, is a rare disease that eventually leads to right heart failure (RHF) and death.[1,2] The 5-year mortality rate of this disease can be as high as 46% if with no proper treatment.[3] However, misdiagnosis and

underdiagnosis of PH-FM are common due to the rarity, lack of awareness, and non-specificity of symptoms of this fatal disease. Therefore, early detection and effective intervention of PH-FM are of paramount importance against RHF in clinical practice.

FM is a rare and benign disorder characterized by proliferation of dense fibrous tissue that eliminates normal mediastinal fat tissue and encases or invades adjacent structures.[4] Most FM patients have a history of infection by *Histoplasma capsulatum* or *Mycobacterium tuberculosis*.[5] Other pathogenic factors include infection by other types of fungi and sarcoidosis.[6,7] The protruding proliferative fibrotic tissues compress or encroach on the mediastinal structures, including bronchus, esophagus, vena cava, and pulmonary vasculature, leading to atelectasis, superior vena cava syndrome (SVCS), PH, and pleural effusion.[8,9]

Chest X-ray radiography (CXR) is an inexpensive and convenient examination approach for PH with availability and accessibility in conventional clinical settings.[10] Previous study indicated that CXR features, including FM dyad (prominent main pulmonary artery and atelectasis) and FM triad (the dyad plus refractory pleural effusion), are important diagnostic clues for PH-FM.[2] However, the accuracy of CXR features for diagnosis of PH-FM remains unknown. Therefore, this study sought to systematically summarize the CXR features of the patients with PH-FM, and to evaluate the accuracy of CXR for PH-FM diagnosis, in the hope to improve the early detection and diagnosis of PH-FM among PH patients.

Methods

Patient recruitment and data collection
This was a retrospective cohort study from Gansu Provincial Hospital. The Strengthening the Reporting of Observational Studies in Epidemiology (STROBE) guidelines were followed when preparing the article. Patients who were 18 years of age or older and in suspicion of PH [estimated pulmonary artery systolic pressure (PASP) >40 mmHg using echocardiography][11] were recruited between October 2014 and October 2020. Diagnosis of PH was confirmed by mean pulmonary artery pressure (mPAP) ≥ 25 mmHg on right heart catheterization (RHC). In addition,

pulmonary arterial hypertension (PAH) was determined as mPAP ≥ 25 mmHg, pulmonary artery wedge pressure ≤ 15 mmHg, and pulmonary vascular resistance (PVR) >3 Wood units on RHC[1] (Figure 1). All the clinical data and CXR findings were collected from the medical records of the patients. Furthermore, the CXR findings had been independently re-evaluated and confirmed by chest computed tomography (CT) under surveillance of two radiologists (Supplementary Table 1). The Ethics Committee of Gansu Provincial Hospital reviewed and approved the study protocol (2020-204) on 15 October 2020 and granted exemption from obtaining informed consent from patients.

Diagnostic criteria of FM in CT
Findings in contrast-enhanced chest CT included devoid of fat tissue, excessive proliferation of fibrotic tissues in the mediastinum, and abnormal compression of mediastinal structures, such as airway and vasculature by soft tissues.[12] Sarcoidosis and tumor were excluded.

### Inclusion and exclusion criteria of the patients
The included patients should have (1) RHC, (2) standard posteroanterior chest radiogram;, and (3) contrast-enhanced chest CT. Patients with congenital heart disease, mediastinal tumor, or incomplete hemodynamic data were excluded.

Variables and definitions
In each CXR, the imaging parameters were assessed and described in accordance with the Glossary of Terms for Thoracic Imaging of the Fleischner Society.[13]

In the CXR of all subjects, five parameters were measured (Supplemental Figure 1):

1. Mediastinal width: the maximum distance from the right to the left upper mediastinum at the aortic bulb level (Supplemental Figure 1(A));[14]
2. Hilar width: the maximum distance from the most lateral visible frontier of hilum to the other lateral frontier (Supplemental Figure 1(B));[10]
3. Prominent right heart border (PRHB): defined as more than 44 mm of the maximum
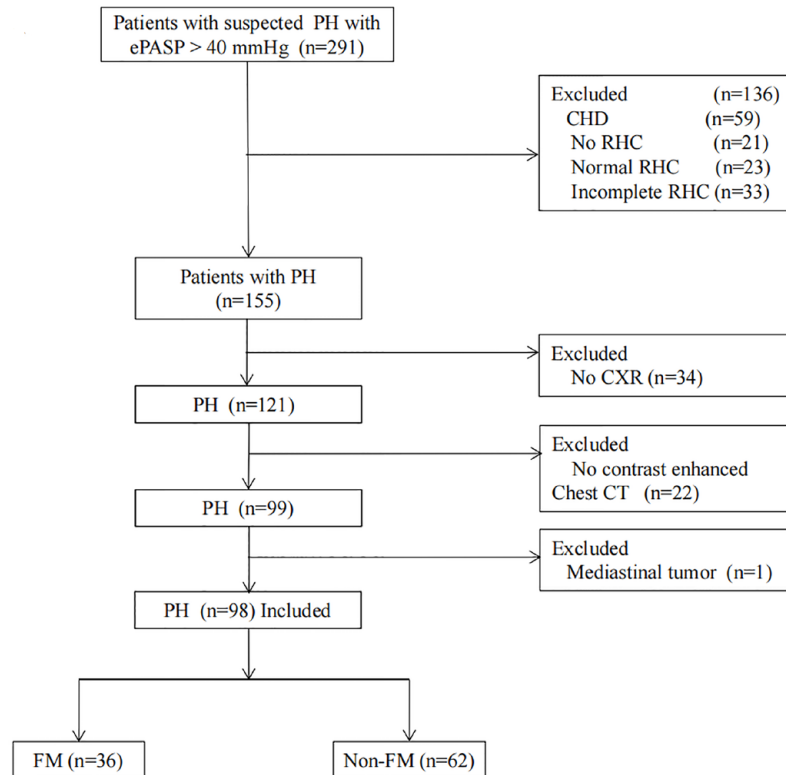
Figure 1. The flowchart of patient selection and exclusion.
CHD, congenital heart disease; CT, computed tomography; CXR, chest X-ray; ePASP, estimated pulmonary artery systolic pressure; FM, fibrosing mediastinitis; PH, pulmonary hypertension; RHC, right heart catheterization.

distance from the right visible boundary of the heart to the midline of the thorax (Supplemental Figure 1(C));[10]

4. Trans-cardiac diameter: the maximum distance from the most lateral point on the right to that on the left cardiac profiles (Supplemental Figure 1(C) and (D));[15]

5. Trans-thoracic diameter: the inside length of the rib cage at the level of the dome of the right hemidiaphragm (Supplemental Figure 1(E));[15]

6. Prominent main pulmonary artery is shown in Supplemental Figure 1(B) and (C);

7. Pleural effusion and atelectasis are shown in Supplemental Figure 1(B) and (C), and are confirmed by chest CT.

Statistical analysis

Normal distribution test was performed for the continuous variables. The continuous variables were presented as mean ± standard deviation (SD) if the data were normally distributed, or as median with interquartile range if the data did not conform to normal distribution. The difference between the groups was examined by either independent t test or one-way analysis of variance followed by the least significant difference comparison method. Categorical data were expressed as numbers with percentages and were compared between groups by Chi-square or Fisher's exact test, as appropriate.

The analyses of univariate logistic regression and receiver operating characteristic curve (ROC) were performed to evaluate the diagnostic specificity and sensitivity of each parameter, and then the predictor with optimal diagnostic accuracy was selected. ROC curves of all independent variables were generated, and the area under the curve (AUC) values of the variables were compared with DeLong test. Because the N-terminal pro-B-type brain natriuretic peptide (NT-proBNP) value did not have normality, log-transformed BNP was considered normality and analyzed. Variables with statistical significance ($p < 0.05$ in independent

t test or one-way analysis of variance) were selected into multivariable logistic regression analysis to determine the factors associated with the risk of PH-FM and to establish a prediction model.

Independent predictors ($p < 0.05$ in the multivariate logistic regression analysis) were included in the construction of a nomogram. The predictive performance of the nomogram was measured by concordance index (c-index), evaluated by ROC analysis, and compared by DeLong test. Internal validation and calibration were performed using a calibration plot with bootstraps of 1000 resamples, which showed the fitting between the observed and nomogram-predicted probability.

Statistical analyses were performed using SPSS 25.0 for Windows, MedCalc 15.2.2 for Windows, and R software (version 4.1.0; R Foundation for Statistical Computing, Vienna, Austria). Two-tailed $p < 0.05$ was considered statistically significant.

Results

Baseline information
Overall, 291 patients were under suspicion of PH according to the results of echocardiography. Of these patients, 98 were diagnosed as PH according to RHC measurement and included in the study (PH-FM: 36, PH-non-FM: 62; Figure 1). The PH-non-FM patients included 9 with idiopathic pulmonary arterial hypertension (IPAH), 3 with connective tissue disease–associated pulmonary arterial hypertension (PAH-CTD), 4 with left-sided heart disease–related PH (PH-LHD), 19 with chronic lung diseases- or chronic hypoxia-associated PH, 19 with CTEPH, and 8 with pulmonary vasculitis (Table 1). The patients with PH-FM were significantly older than those with PH-non-FM (66.00 ± 10.50 *versus* 56.00 ± 23.00 years, $p < 0.001$, Table 1). There was no gender difference between the two groups ($p = 0.690$, Table 1). Significantly, higher prevalence of tuberculosis (44.4% *versus* 3.2%; $p < 0.001$) was found in the PH-FM patients than that in the PH-non-FM patients. The morbidities of hypertension (41.7% *versus* 25.8%; $p = 0.104$), diabetes (11.1% *versus* 9.7%; $p = 0.904$), and chronic obstructive pulmonary disease (COPD) (38.9% *versus* 21.0%; $p = 0.056$) were similar between the two groups (Table 1). Moreover, the PH-non-FM patients had significantly higher

NT-proBNP levels than the PH-FM patients (306.50 ± 728.25 *versus* 988.00 ± 2714.00 pg/ml, $p = 0.020$). Regarding hemodynamics, the PH-non-FM patients had higher right atrial pressure (RAP, 4.00 ± 6.00 *versus* 3.00 ± 2.75 mmHg, $p = 0.002$) than the PH-FM patients, although no significant difference in the other hemodynamic parameters was found between the two groups (Table 1).

Radiographical findings
As shown in Table 2, 18 CXR features were identified and summarized. The frequencies of widened mediastinum ($p = 0.127$), right paratracheal stripe ($p = 0.133$), hilar enlargement ($p = 0.524$), left pleural effusion ($p = 0.737$), unilateral pleural effusion ($p = 0.079$), prominent main pulmonary artery ($p = 0.092$), right descending pulmonary artery (RDPA) ($p = 0.913$), and cardiac enlargement ($p = 0.067$) were not significantly different between the two groups. By contrast, consolidation ($p < 0.001$), nodules ($p = 0.003$), calcification ($p = 0.004$), interlobular septal thickening ($p = 0.013$), interstitial reticulation ($p = 0.007$), atelectasis ($p < 0.001$), pleural effusion ($p = 0.0001$), right pleural effusion ($p = 0.042$), and bilateral pleural effusion ($p = 0.019$) were more prevalent in patients with PH-FM than in patients with PH-non-FM. Conversely, the incidence of PRHB ($p = 0.020$) was significantly declined in patients with PH-FM compared with that in patients with PH-non-FM.

Accuracy of CXR for diagnosing PH-FM
An ROC analysis was performed to assess the abilities of imaging parameters to distinguish PH-FM from PH-non-FM. The ROC analysis revealed that atelectasis had the largest AUC [0.720, 95% confidence interval (CI): 0.634–0.806] among all the CXR imaging parameters (Figure 2, Supplementary Figure 2, and Supplementary Table 2). Supplemental Table 3 showed the sensitivity, specificity, positive predictive value (PPV), negative predictive value (NPV), and likelihood ratio (LR), which were calculated to assess the predictive value of each CXR feature.

Multivariate logistic regression
Univariate logistic regression analysis identified that age, tuberculosis, NT-proBNP, natural logarithmic NT-proBNP (lnBNP), RAP, atelectasis,

**Table 1.** Baseline characteristics of patients.

	PH-FM (*n* = 36)	PH-non-FM (*n* = 62)	*p* value
Age (years)	66.00 (10.50)	56.00 (23.00)	0.001
Male, *n* (%)	16 (44.44)	25 (40.32)	0.690
Comorbidity, *n* (%)			
Hypertension	15 (41.7)	16 (25.8)	0.104
COPD	14 (38.9)	13 (21.0)	0.056
Diabetes	4 (11.1)	6 (9.7)	0.904
Tuberculosis	16 (44.4)	2 (3.2)	<0.001
PH group, *n* (%)			
Group 1	N/A	12 (19.4)	N/A
IPAH	N/A	9 (14.5)	N/A
CTD	N/A	3 (4.8)	N/A
Group 2			
Left heart disease	N/A	4 (6.5)	N/A
Group 3			
Chronic lung disease/hypoxia	N/A	19 (30.6)	N/A
Group 4	N/A	27 (43.5)	N/A
CTEPH	N/A	19 (30.6)	N/A
Vasculitis	N/A	8 (12.9)	N/A
Group 5			
FM	36 (100.0)	N/A	N/A
NT proBNP, pg/ml	306.50 (728.25)	988.00 (2714.00)	0.020
lnNT proBNP, pg/ml	6.08 ± 1.18	6.72 ± 1.58	0.038
Hemodynamics			
mPAP, mmHg	39.50 (9.75)	41.00 (20.50)	0.883
RAP, mmHg	3.00 (2.75)	4.00 (6.00)	0.002
PCWP, mmHg	7.00 (4.50)	8.00 (7.00)	0.177
CO, l/min	4.45 (1.13)	4.35 (1.85)	0.249
CI, l/min/m^2	3.00 (0.86)	2.70 (0.99)	0.105
PVR, Wood units	6.81 (3.08)	7.27 (5.63)	0.805
SvO$_2$, %	61.50 (9.75)	59.00 (11.00)	0.142

CI, cardiac index; CO, cardiac output; COPD, chronic obstructive pulmonary disease; CTD, connective tissue disease; CTEPH, chronic thromboembolic pulmonary hypertension; FM, fibrosing mediastinitis; IPAH, idiopathic pulmonary arterial hypertension; lnBNP, natural logarithm of NT-proBNP; mPAP, mean pulmonary arterial pressure; NA, not applicable; NT-proBNP, N-terminal pro-B-type brain natriuretic peptide; PCWP, pulmonary capillary wedge pressure; PH-FM, pulmonary hypertension caused by fibrosing mediastinitis; PVR, pulmonary vascular resistance; RAP, right atrial pressure; SvO$_2$, mixed venous oxygen saturation.

Table 2. CXR findings in patients with PH caused by fibrosing mediastinitis.

CXR findings	PH-FM (n = 36)	PH-non-FM (n = 62)	p value
Focal mediastinal abnormalities			
Widened mediastinum	9 (25)	8 (13)	0.127
Right paratracheal stripe	2 (6)	0 (0)	0.133
Hilar enlargement	5 (14)	6 (10)	0.524
Parenchymal abnormalities			
Atelectasis	17 (47)	2 (3)	<0.001
Consolidation	33 (92)	32 (52)	<0.001
Nodules	31 (86)	35 (56)	0.003
Calcification	27 (75)	28 (45)	0.004
Interstitial disease lung			
Interlobular septal thickening	35 (97)	47 (76)	0.013
Interstitial reticulation	29 (81)	33 (53)	0.007
Pleural effusion	31 (86)	29 (48)	0.0001
Right pleural effusion	9 (25)	6 (10)	0.042
Left pleural effusion	3 (8)	5 (8)	0.737
Unilateral pleural effusion	12 (33)	11 (18)	0.079
Bilateral pleural effusion	19 (53)	18 (29)	0.019
Signs of PH			
Prominent main pulmonary artery	9 (25)	26 (42)	0.092
RDPA	12 (33)	20 (32)	0.913
Cardiac signs			
PRHB	11 (31)	34 (55)	0.020
Cardiac enlargement	26 (72)	54 (87)	0.067

CXR, chest X-radiography; PH-FM, pulmonary hypertension caused by fibrosing mediastinitis; PRHB, prominent right heart border; RDPA, right descending pulmonary artery.
Data are number (%).

consolidation, nodules, calcification, pleural effusion, right pleural effusion, bilateral pleural effusion, interlobular septal thickening, interstitial reticulation, and PRHB were significantly different between the two groups, which were selected for multivariate regression analysis. Among these factors, the multivariate regression analysis based on a forward LR indicated that tuberculosis [odds ratio (OR) = 29.40, 95% CI: 3.7–232.4, $p = 0.001$], lnBNP (OR = 0.649, 95% CI: 0.4–0.99, $p = 0.048$), atelectasis (OR = 18.56, 95% CI: 2.9–119.5, $p = 0.002$), pleural effusion (OR = 9.83, 95% CI: 2.1–45.3, $p = 0.003$), and PRHB (OR = 0.22, 95% CI: 0.1–0.9, $p = 0.040$) were independent predictive factors for PH-FM (Table 3 and Supplementary Table 4).
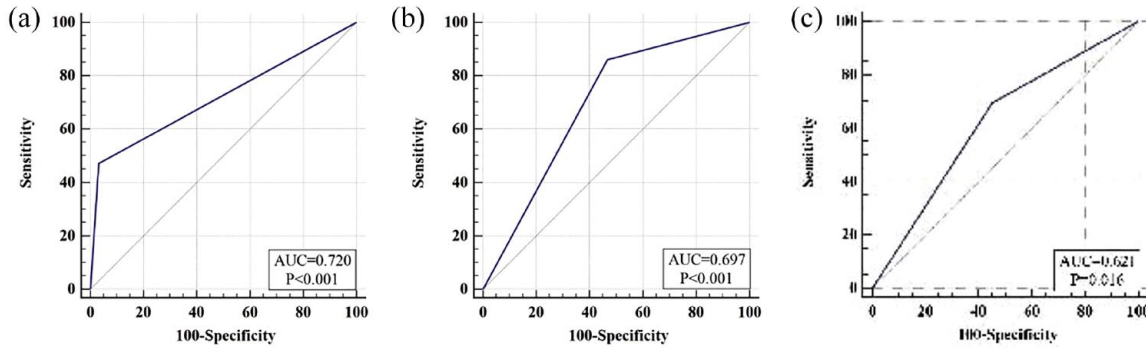
Figure 2. The power for predicting fibrosing mediastinitis using ROC curves: (a) atelectasis, (b) pleural effusion, and (c) PRHB.
AUC, area under the curve; PRHB, prominent right heart border; ROC, receiver operator characteristic.

The logistic regression formula was: $Logistic(P) = ln\,(P/(1-P)) = 0.091 + 2.921\,Atelectasis + 2.285\,Effusion + 3.381\,Tuberculosis - 1.495\,PRHB - 0.432\,lnBNP$ (atelectasis = 1 if present, 0 absent; effusion = 1 present, 0 absent; tuberculosis = 1 present, 0 absent; PRHB = 0 present, 1 absent; lnBNP refers to the natural logarithm of the BNP value. PRHB indicates that the maximum distance from the midline to the right heart border is more than 44 mm. The cutoff point was 0.341.)

Based on these results (Table 3), a prediction model for PH-FM was established, with a sensitivity of 91.7% and a specificity of 83.9% (AUC = 0.922, 95% CI: 0.861–0.983) (Table 4). The ROCs showed the superior power of the prediction model in distinguishing PH-FM from PH-non-FM. Then, to ensure that there was no multicollinearity, feature selection was carried out by calculating tolerance and variance inflation factor (VIF) of each variable in the subset of statistical predictors from the stepwise regression results. It turned out that the tolerance was more than 0.1, and VIF was substantially less than 10 in the current study (Supplemental Table 5), indicating no collinearity among the independent variables.

Table 3. Multivariate logistic regression analyses based on a forward likelihood ratio stepwise selection procedure.

	OR	95% CI	*p* value
Atelectasis	18.56	2.9–119.5	0.002
Pleural effusion	9.83	2.1–45.3	0.003
Tuberculosis	29.40	3.7–232.4	0.001
PRHB	0.22	0.1–0.9	0.040
lnBNP	0.649	0.4–0.99	0.048

CI, confidence interval; lnBNP, the natural logarithm of N-terminal pro-B-type brain natriuretic peptide; OR, odds ratio; PRHB, prominent right heart border.

Development of nomogram and internal validation
Nomogram for PH-FM was developed based on the analysis results (Figure 3(a)). To further examine the stability of the nomogram, an internal validation was conducted, and then the C-index and AUC values were calculated (Figure 3(b)). As shown in Figure 3(c), when the cutoff point was 0.341 for predicting the risk of PH-FM in PH patients, the combination of five factors

Table 4. The sensitivity and specificity of atelectasis, pleural effusion, tuberculosis, PRHB, and lnBNP.

Sensitivity, % (95% CI)	Specificity, % (95% CI)	Positive LR (95% CI)	Negative LR (95% CI)	AUC
91.7 (77.5–98.2)	83.9 (72.3–92.0)	5.68	0.099	0.922 (0.861–0.983)

AUC, area under curve; CI, confidence interval; lnBNP, the natural logarithm of N-terminal pro-B-type brain natriuretic peptide; LR, likelihood ratio; PRHB, prominent right heart border.
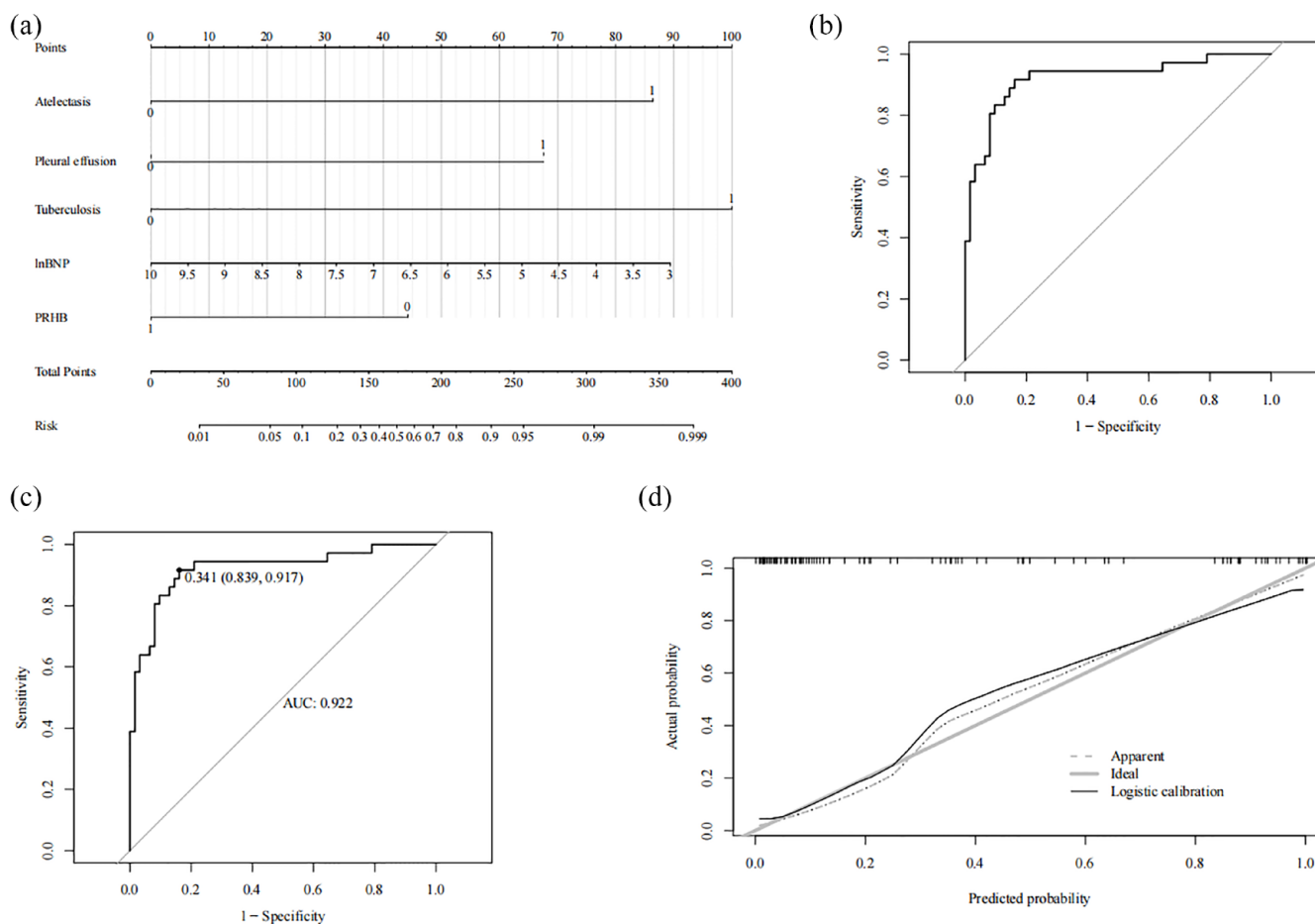
Figure 3. Nomogram for multivariate logistic regression. (a) The nomogram scores of the five features (tuberculosis, lnBNP, PRHB, atelectasis, and pleural effusion) predicting pulmonary hypertension in patients with fibrosing mediastinitis. (b) Internal validation of the nomogram using ROC curve. (c) The nomogram was calibrated for the probability of pulmonary hypertension in patients with fibrosing mediastinitis (bootstrap 1000 repetitions). (d) Using cutoffs for the predicted probability of fibrosing mediastinitis in specific combinations of true-positive rate (sensitivity) and false-positive rate (1-specificity). The AUC is 0.922.
AUC, area under the curve; CI, confidence interval; lnBNP, the natural logarithm of N-terminal pro-B-type brain natriuretic peptide; PRHB, prominent right heart border; ROC, receiver operator characteristic.

could reach the specificity of 0.839 and the sensitivity of 0.917, with the AUC being 0.922 (95% CI: 0.861–0.983). The established nomograms had a C-index of 0.922 (95% CI: 0.860–0.983) and were well calibrated (Figure 3(d)).

Discussion

This retrospective and observational study demonstrated the value of CXR in screening PH-FM patients among patients with PH. The results suggest that the CXR features may facilitate identification of PH-FM based on clinical information. Specifically, the most typical features of PH-FM on CXR were atelectasis, pleural effusion, and PRHB. If clinical information, such as history of tuberculosis and lnBNP value, was added, the accuracy in prediction of PH-FM could be improved. The predictive model composed of these five factors had excellent calibration and discrimination, thereby facilitating early identification and diagnosis of PH-FM among PH patients in the primary hospital (Figure 4).

FM is a rare, benign but fatal disease characterized by mediastinal fibrotic tissue proliferation induced by histoplasmosis or tuberculosis in most cases. The proliferative fibrotic tissue compresses airway and vasculature, thereby leading to PH, RHF, and death.[3–5,8] In this study, the patients
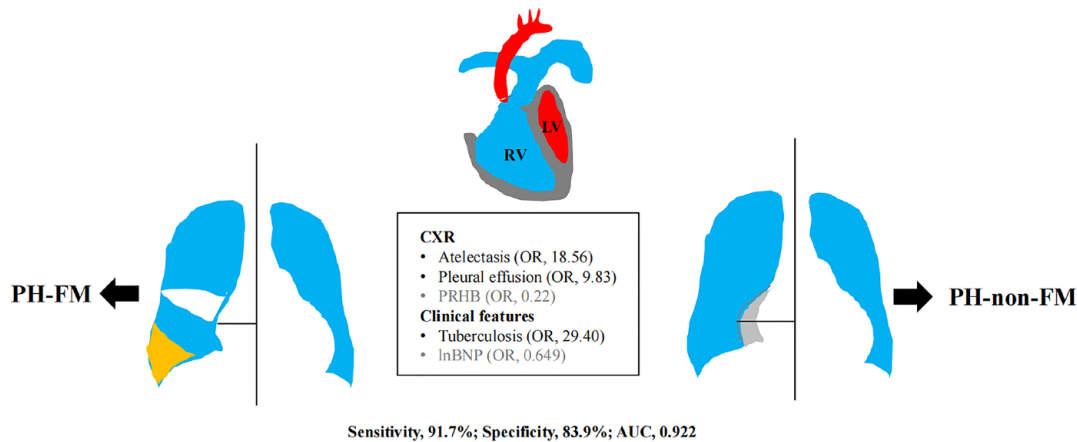
Figure 4. CXR facilitate screening for PH-FM.
CXR, chest X-ray; LV, left ventricle; PH-FM, pulmonary hypertension caused by fibrosing mediastinitis; PRHB, prominent right heart border; RV, right ventricle; white, atelectasis; yellow, pleural effusion.

with PH-FM were older than those with PH-non-FM. Nearly half of the FM cases in this study were caused by tuberculosis. The RAP and NT-proBNP levels in patients with PH-non-FM were higher than those in patients with PH-FM, indicating that the PH-non-FM patients had exacerbated dysfunctions in the right heart compared with those with PH-FM.

Previously, the imaging features of the patients with FM have been reported to include mediastinal widening, hilar enlargement, and right side parabronchial signs.[12,16] However, in this study, there were no significant differences in these parameters between the PH-FM and PH-non-FM patients. This could be ascribed to the greater incidence of hypoxia and pulmonary parenchymal abnormalities in the non-FM patients. However, atelectasis, consolidation, nodules, calcification, interlobular septal thickening, grid-like lesions, and pleural effusion were more prevalent to patients with PH-FM, and these observations were related to the pathological process of FM.[8,12,16] The enlargements in the main pulmonary artery and RDPA were the imaging features of PH,[10] and there is no difference in these features between the two groups of patients.

Interestingly, multiple regression analysis revealed that atelectasis, pleural effusion, tuberculosis, lnBNP, and PRHB were associated with PH-FM (Figure 4). As a matter of fact, these parameters are related to the special pathophysiological process of FM.[4,8,17] For example, atelectasis is related to bronchial compression complicated by FM, for which tuberculosis is the special trigger.[18,19] Indeed, our results have demonstrated that atelectasis has an incidence up to 47% in the PH-FM group, almost half of which have the history of tuberculosis. Our results were comparable to other studies reporting that the incidence of atelectasis in tuberculosis-caused FM ranges from 37% to 50%.[3,18,20] By contrast, the atelectasis that occurred in two patients of the PH-non-FM group was caused by obstructive pneumonia without bronchial compression and stenosis, and their symptoms were improved following anti-inflammatory treatments.

However, among the 36 patients with PH-FM recruited in this study, 31 (86%) had pleural effusions and 19 (53%) were bilaterally afflicted, which agrees to the notion that the pleural effusion in the PH-FM patients was mainly caused by pulmonary vein stenosis (PVS).[9,21] Indeed, among the 30 patients with FM-caused PVS recruited in our prior study, 19 suffered from refractory pleural effusion; Furthermore, 17 out of the 19 patients with refractory pleural effusion were relieved by pulmonary vein angioplasty.[21] Admittedly, the PH-induced RHF is also involved to varying extents in the formation of pleural effusion in the patients with PH-FM. By contrast, 29 (48%) patients in the PH-non-FM group had pleural effusions and 18 (29%) had bilateral afflictions. This was in consistency with the

incidence of pleural effusions in PAH, IPAH/HPAH (heritable PAH), and PH-CTD, the diseases belonging to PH-non-FM and predominantly caused by RHF.[22,23] These results suggested that the pleural effusion in the patients with PH-non-FM was primarily caused by RHF.

It is notable that prominent main PA, atelectasis, and pleural effusion have been proposed as FM triad to facilitate the screening of PH-FM.[8] PRHB demonstrated a negative correlation to PH-FM, being consistent with lower NT-proBNP and RAP levels in PH-FM patients than those in PH-non-FM patients.

Limitations
There were limitations in this study. First, this study was a single-center, retrospective study with a small sample size, which may increase the bias and limit generalization of the findings. Moreover, the individual variabilities within and between the study groups may influence the comparability and objectivity of the data. Therefore, a prospective, randomized, multi-center study with a large sample size is warranted to corroborate the identified correlations.

Conclusion
In conclusion, a combination of atelectasis, pleural effusion, PRHB, tuberculosis, and lnBNP is more accurate for predicting PH-FM among PH patients, thereby facilitating identification of PH-FM and improving diagnosis of this rare but fatal disease.

Declarations

Author contributions
Mingfang Zhou: Formal analysis; Writing – original draft; Writing – Review & Editing.

Bo Li: Writing – original draft; Writing – Review & Editing.

Yaling Chen: Writing – review & editing.

Aqian Wang: Writing – review & editing.

Yining Zhu: Methodology.

Yu Li: Writing – review & editing.

Hongling Su: Writing – review & editing.

Jingchun Fan: Methodology.

Yan Zhang: Conceptualization; Writing – review & editing.

Yunshan Cao: Conceptualization; Funding acquisition; Writing – review & editing.

ORCID iDs
Bo Li (iD) https://orcid.org/0000-0002-5281-3295

Yunshan Cao (iD) https://orcid.org/0000-0001-8463-1093

Supplemental material
Supplemental material for this article is available online.

References
1. Galie N, Humbert M, Vachiery JL, *et al.* 2015 ESC/ERS guidelines for the diagnosis and treatment of pulmonary hypertension: the joint task force for the diagnosis and treatment of pulmonary hypertension of the

European Society of Cardiology (ESC) and the European Respiratory Society (ERS): endorsed by: Association for European Paediatric and Congenital Cardiology (AEPC), International Society for Heart and Lung Transplantation (ISHLT). *Eur Heart J* 2016; 37: 67–119.

2. Wang A, Su H, Duan Y, *et al.* Pulmonary hypertension caused by fibrosing mediastinitis. *JACC Asia* 2022; 2: 218–234.

3. Seferian A, Steriade A, Jais X, *et al.* Pulmonary hypertension complicating fibrosing mediastinitis. *Medicine* 2015; 94: e1800.

4. Manyeruke FD, Perumal R, Symons G, *et al.* Idiopathic fibrosing mediastinitis. *Afr J Thorac Crit Care Med* 2021; 27: 60–62.

5. Kobayashi Y, Ishiguro T, Takaku Y, *et al.* Clinical features of fibrosing mediastinitis in Japanese patients: two case reports and a literature review. *Intern Med* 2021; 60: 3765–3772.

6. Ahmed S, Hameed M, Thomas MM, *et al.* Ptosis and miosis associated with fibrosing mediastinitis. *Am J Case Rep* 2021; 22: e927556.

7. Rishi AR, Zurob A, Williams C, *et al.* Complete lung collapse as a rare complication of sarcoidosis-associated mediastinal lymphadenopathy. *Respirol Case Rep* 2021; 9: e00739.

8. Cao YS, Duan YC and Su HL. Advances in diagnosis and therapy of pulmonary vascular stenosis induced by fibrosing mediastinitis. *Zhonghua Xin Xue Guan Bing Za Zhi* 2020; 48: 823–830.

9. Yang S, Wang J, Li J, *et al.* Refractory pleural effusion as a rare complication of pulmonary vascular stenosis induced by fibrosing mediastinitis: a case report and literature review. *J Int Med Res* 2021; 49: 3000605211010073.

10. Mirsadraee M, Nazemi S, Hamedanchi A, *et al.* Simple screening of pulmonary artery hypertension using standard chest x ray: an old technique, new landmark. *Tanaffos* 2013; 12: 17–22.

11. Rudski LG, Lai WW, Afilalo J, *et al.* Guidelines for the echocardiographic assessment of the right heart in adults: a report from the American Society of Echocardiography endorsed by the European Association of Echocardiography, a registered branch of the European Society of Cardiology, and the Canadian Society of Echocardiography. *J Am Soc Echocardiogr* 2010; 23: 685–713. Quiz 786.

12. Garin A, Chassagnon G, Tual A, *et al.* CT features of fibrosing mediastinitis. *Diagn Interv Imaging* 2021; 102: 759–762.

13. Hansell DM, Bankier AA, MacMahon H, *et al.* Fleischner society: glossary of terms for thoracic imaging. *Radiology* 2008; 246: 697–722.

14. Woodring JH and King JG. Determination of normal transverse mediastinal width and mediastinal-width to chest-width (M/C) ratio in control subjects: implications for subjects with aortic or brachiocephalic arterial injury. *J Trauma* 1989; 29: 1268–1272.

15. Schmidt HC, Kauczor HU, Schild HH, *et al.* Pulmonary hypertension in patients with chronic pulmonary thromboembolism: chest radiograph and CT evaluation before and after surgery. *Eur Radiol* 1996; 6: 817–825.

16. Tabotta F, Ferretti GR, Prosch H, *et al.* Imaging features and differential diagnoses of non-neoplastic diffuse mediastinal diseases. *Insights Imaging* 2020; 11: 111.

17. Loyd JE, Tillman BF, Atkinson JB, *et al.* Mediastinal fibrosis complicating histoplasmosis. *Medicine* 1988; 67: 295–310.

18. Hu Y, Qiu JX, Liao JP, *et al.* Clinical manifestations of fibrosing mediastinitis in Chinese patients. *Chin Med J* 2016; 129: 2697–2702.

19. Atasoy C, Fitoz S, Erguvan B, *et al.* Tuberculous fibrosing mediastinitis: CT and MRI findings. *J Thorac Imaging* 2001; 16: 191–193.

20. Liu T, Gao L, Xie S, *et al.* Clinical and imaging spectrum of tuberculosis-associated fibrosing mediastinitis. *Clin Respir J* 2018; 12: 1974–1980.

21. Duan YC, Su HL, Wei R, *et al.* Short-term efficacy and perioperative safety of catheter-based intervention for pulmonary vein stenosis caused by fibrosing mediastinitis. *Zhonghua Xin Xue Guan Bing Za Zhi* 2022; 50: 55–61.

22. Tang KJ, Robbins IM and Light RW. Incidence of pleural effusions in idiopathic and familial pulmonary arterial hypertension patients. *Chest* 2009; 136: 688–693.

23. Brixey AG and Light RW. Pleural effusions occurring with right heart failure. *Curr Opin Pulm Med* 2011; 17: 226–231.